Article

Cell Reports

Cadherin-7 Regulates Mossy Fiber Connectivity in the Cerebellum

Graphical Abstract

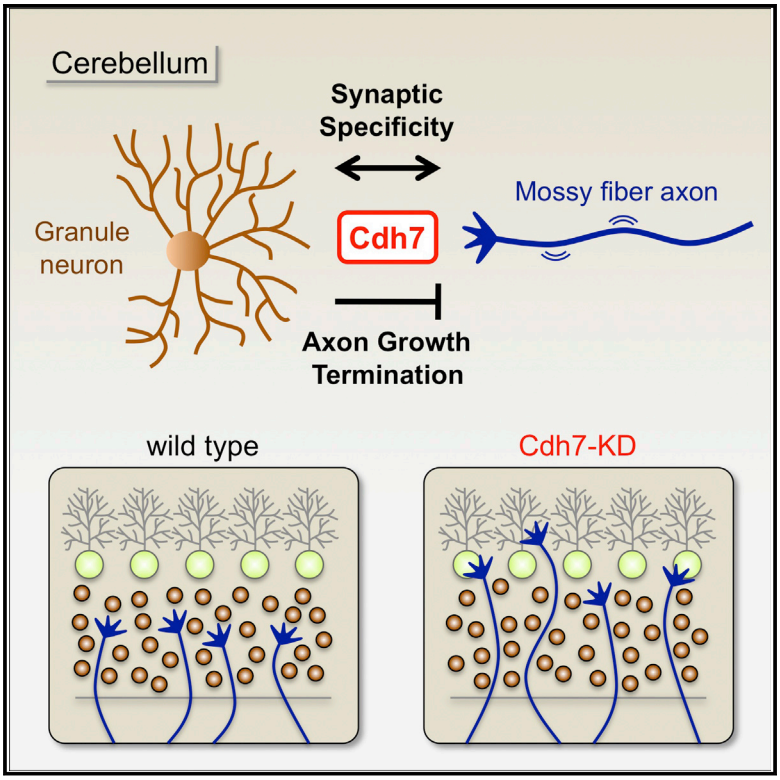

Highlights

Cdh7 is expressed in mossy fiber PN neurons and cerebellar neurons

Mature granule neurons diminish the growth potential of PN axons through Cdh7

Cdh7 selectively mediates synapse formation between PN neurons and granule neurons

Loss of Cdh7 in PN neurons impairs the connectivity of PN axons in the cerebellum

Authors

Ken-ichiro Kuwako, Yoshinori Nishimoto, ..., Hirotaka James Okano, Hideyuki Okano

Correspondence

kuwako@z2.keio.jp (K.-i.K.),
hidokano@a2.keio.jp (H.O.)

In Brief

Spatiotemporally orchestrated mechanisms for terminating axonal growth and forming specific synapses are essential in establishing precise neural connectivity. Kuwako et al. demonstrate that cadherin-7 critically regulates the connectivity of the cerebellar mossy fiber circuit by mediating growth inhibition of innervating mossy fiber axons and selective synapse formation between mossy fiber neurons and cerebellar granule neurons. This study reveals that a single cell-surface receptor may play a dual role in axonal growth termination and synaptic specificity to develop precise wiring.

Kuwako et al., 2014, Cell Reports 9, 311–323
October 9, 2014 ©2014 The Authors
http://dx.doi.org/10.1016/j.celrep.2014.08.063

Cell Reports
Article

Cadherin-7 Regulates Mossy Fiber Connectivity in the Cerebellum

Ken-ichiro Kuwako,[1,*] Yoshinori Nishimoto,[1] Satoshi Kawase,[1] Hirotaka James Okano,[2] and Hideyuki Okano[1,*]
[1]Department of Physiology, Keio University School of Medicine, 35 Shinanomachi, Shinjuku-ku, Tokyo 160-8582, Japan
[2]Division of Regenerative Medicine, Jikei University School of Medicine, 3-25-8 Nishi-Shinbashi, Minato-ku, Tokyo 105-8461, Japan
*Correspondence: kuwako@z2.keio.jp (K.-i.K.), hidokano@a2.keio.jp (H.O.)
http://dx.doi.org/10.1016/j.celrep.2014.08.063

SUMMARY

To establish highly precise patterns of neural connectivity, developing axons must stop growing at their appropriate destinations and specifically synapse with target cells. However, the molecular mechanisms governing these sequential steps remain poorly understood. Here, we demonstrate that cadherin-7 (Cdh7) plays a dual role in axonal growth termination and specific synapse formation during the development of the cerebellar mossy fiber circuit. Cdh7 is expressed in mossy fiber pontine nucleus (PN) neurons and their target cerebellar granule neurons during synaptogenesis and selectively mediates synapse formation between those neurons. Additionally, Cdh7 presented by mature granule neurons diminishes the growth potential of PN axons. Furthermore, knockdown of Cdh7 in PN neurons in vivo severely impairs the connectivity of PN axons in the developing cerebellum. These findings reveal a mechanism by which a single bifunctional cell-surface receptor orchestrates precise wiring by regulating axonal growth potential and synaptic specificity.

INTRODUCTION

Precise synaptic connections in the nervous system are crucial for the establishment of functional neural circuits. During neural development, once the growing axons arrive at their destinations, neurons halt the axonal growth program and select the appropriate target cells to form specific synapses. Because axons must be effectively stabilized to develop synapses soon after they connect to their ultimate target cells, axon-target connection and axonal growth termination should be closely orchestrated in a spatiotemporal manner. Although various mechanisms have been explored in the control of synaptic specificity, including mutual recognition and elimination (Sanes and Yamagata, 2009; Shen and Scheiffele, 2010), the molecules that have been identified as being involved in synaptic specificity remain limited, especially in mammals. In addition, how neurons correctly terminate axonal movement in their target regions remains obscure in most circuits. Accordingly, a coupled mechanism establishing specific synaptic connections and terminating axonal growth during neural development has yet to be determined.

The cerebellum is an excellent model for studying circuit connectivity because of its well-characterized simple circuits that consist of a small number of neuronal cell types (Altman and Bayer, 1997). Climbing and mossy fibers, the two afferent networks, convey information to the cerebellum. Climbing fibers, which emerge from the inferior olivary nucleus (IO) neurons in the caudal hindbrain, selectively and directly synapse with Purkinje cells in the cerebellar cortex, whereas mossy fibers, which originate from several distinct neuronal types, such as PN neurons, innervate granule neurons and Golgi cells in the granule cell layer (GCL) (Figures 1A and 1B). Although previous studies have revealed the morphological features of climbing and mossy fibers in the developing cerebellum in great detail (Mason and Gregory, 1984; Sugihara, 2005), the molecular mechanisms establishing the precise connections of the cerebellar afferent fibers remain largely unknown.

Among the mossy fiber circuits, development of the pontocerebellar circuit between pontine nucleus (PN) neurons and granule neurons has been intensely studied. Growing PN axons project from the basilar pons to the cerebellum (Figure 1C). After arriving at the cerebellar cortex around birth, PN axons greatly decrease their growth and never enter the most apical layer of the developing cerebellar cortex, the external granule cell layer (EGL), where immature granule cells proliferate (Ashwell and Zhang, 1992; Manzini et al., 2006). Thus, PN axons wait below the EGL for granule cells to differentiate into neurons and migrate inward to form the internal granule cell layer (IGL). Differentiated granule neurons start to migrate into the IGL during the middle of the first postnatal week and complete their migration by the third postnatal week (Altman and Bayer, 1997). During this period, some PN axons transiently contact the Purkinje cells. Based on their morphological changes in the IGL, PN axons also continue growing to some degree, presumably to translocate from the Purkinje cells to granule neurons (Mason and Gregory, 1984; Kalinovsky et al., 2011; White and Sillitoe, 2013). Eventually, by the third postnatal week, PN axons stop growing and establish synaptic connections with granule neurons and Golgi cells in the IGL (i.e., the future GCL).

A heparin-binding factor-dependent "stop" signal from immature granule cells in the EGL may serve as a potent initial brake for PN axons that enter the cerebellar cortex (Manzini et al., 2006). However, the mechanism that terminates the axonal

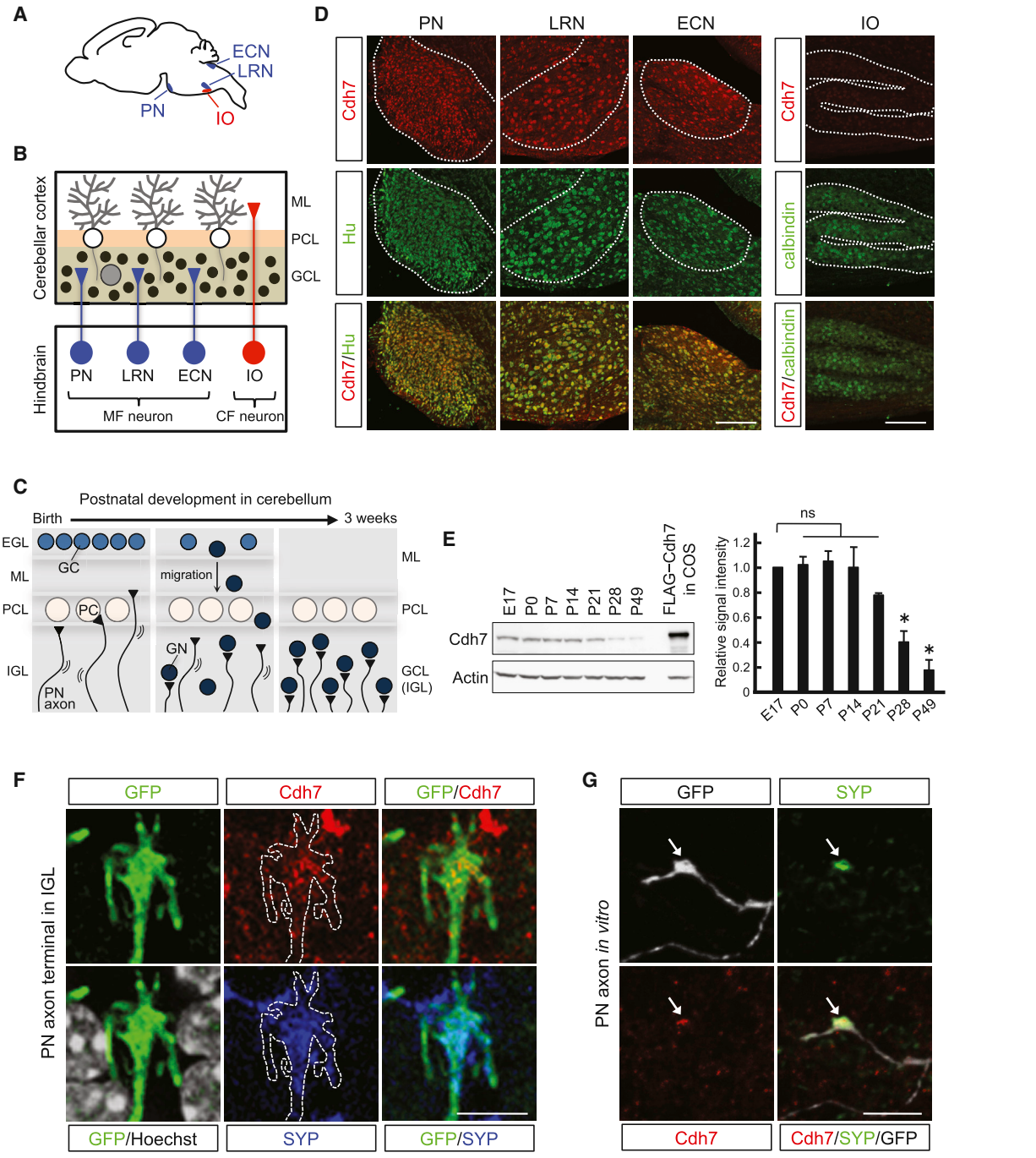

Figure 1. Cdh7 Is Selectively Expressed in Mossy Fiber Neurons

(A and B) Schematic representations of the locations of the neuronal nuclei (A) and the circuits (B) of mossy fiber (MF) and climbing fiber (CF) neurons. Black circle, granule neuron; gray circle, Golgi cell; white circle, Purkinje cell.

(C) Scheme of the development of the pontocerebellar circuit. PN axons arrive at the developing cerebellum around birth, when granule cells (GC) still proliferate in the EGL. Some PN axons transiently contact Purkinje cells (PC). Shortly thereafter, granule cells differentiate into granule neurons (GN) in the EGL and migrate toward the IGL. By the third postnatal week, the contacts between PN axons and Purkinje cells are eliminated, all granule neurons settle in the IGL, and the specific pontocerebellar circuit connections are established. For additional details, refer to Figure S4J.

(D) Sections of P14 hindbrain were immunostained with antibodies against Cdh7 and neuronal markers (Hu and calbindin). The dotted lines indicate the margin of each neuronal nucleus.

(E) Western blot analysis of Cdh7 in PN in vivo. The signal intensities of Cdh7 are normalized to that of actin, and the normalized value of the E17 sample was set at 1.0. The data represent the mean ± SEM of three mice. *$p < 0.01$: E17 versus P28 or P49; ns, not significant.

(legend continued on next page)

growth of PN neurons at the later stage in the IGL, where PN axons ultimately settle and form synapses with their target cells, has not been identified. Purkinje cell-derived BMP4 eliminates erroneous connections between PN axons and Purkinje cells (Kalinovsky et al., 2011). In addition to this error-correction mechanism, unidentified positive signal(s) that selectively connect PN axons to granule neurons may be a key mechanism in establishing the circuit connectivity in the pontocerebellar system (Manzini et al., 2006; Kalinovsky et al., 2011).

In the present study, we have identified Cadherin-7 (Cdh7) as a mediator of synaptic specificity in the pontocerebellar circuit. We also provide evidence suggesting that Cdh7 is involved in the growth termination of PN axons in the IGL. These findings indicate that Cdh7 may spatiotemporally orchestrate the axon-target connection and the axonal growth termination of mossy fiber neurons.

RESULTS

Cdh7 Is Expressed in Mossy Fiber Neurons, but Not in Climbing Fiber Neurons

In *Sema6a*-deficient mice, many granule neurons are abnormally located in the molecular layer (ML) because of migration defects (Kerjan et al., 2005). Nevertheless, mossy fibers synapse with those ectopic granule neurons, suggesting a cell type-based target recognition mechanism in mossy fiber neurons. In addition, even in culture, granule neurons preferentially form synapses with PN axons rather than IO axons, indicating that a cell-surface-associated mechanism is involved in this specific connection (Ito and Takeichi, 2009). Although PN and IO neurons largely share regulatory and molecular machinery during circuit formation (Sotelo and Chédotal, 2013), the axons of PN and IO neurons form synapses exclusively and selectively with their target neurons in the cerebellum at almost the same developmental stage (Mason and Gregory, 1984; Sotelo, 2004). Based on this evidence, we hypothesized that regulators of synaptic specificity in PN neurons might be synapse membrane proteins, especially cell adhesion molecules, that were specifically expressed in PN neurons, but not in IO neurons, at the synaptogenic stage. Thus, to identify the molecule(s) responsible for the synaptic specificity of PN neurons, we first performed a transcriptome analysis based on DNA microarrays using high-purity tissue samples from the PN and IO, which were collected by laser microdissection at postnatal day 12 (P12). Among more than 8,000 genes categorized under the Gene Ontology (GO) term "cell adhesion (GO:0007155)," we identified cell adhesion genes that were specifically expressed in PN neurons (Table S1). We next performed small hairpin RNA (shRNA)-mediated in vivo knockdown of PN-specific cell adhesion molecules to examine the connectivity of PN axons in the cerebellum. Based on preliminary results from this experiment, we hypothesized that Cdh7, a classic type II cadherin specifically expressed in PN neurons (Table S1), would be a strong candidate for regulating the synaptic specificity of PN neurons.

To explore the role of Cdh7 in the synaptic specificity of PN neurons, we first examined the expression of Cdh7 in mossy fiber and climbing fiber neurons by immunohistochemistry using a specific antibody against Cdh7 (Figures S1A–S1D). At P14, Cdh7 was highly expressed in PN neurons (Figure 1D; Figure S1F). Interestingly, Cdh7 was also expressed in the other mossy fiber neurons, including those of the lateral reticular nucleus (LRN) and external cuneate nucleus (ECN) (Figures 1A, 1B, and 1D). In contrast, and consistent with the DNA microarray analysis (Table S1), the expression level of Cdh7 in IO neurons was low compared with that in the mossy fiber neurons (Figure 1D). Cdh7 was consistently expressed in PN neurons at least from embryonic day 17 (E17) to P14, suggesting that Cdh7 expression remains high in PN neurons during synaptogenesis (Figure 1E; Figure S1E). We next examined the localization of Cdh7 in the axon terminal of PN neurons. To label PN axons in vivo, green fluorescent protein (GFP) was expressed in PN neurons by in utero electroporation. At P14, Cdh7 clearly localized in the "rosette" of PN axon terminals in the IGL, a core structure that forms a large synapse complex with granule neurons and Golgi cells and contains presynaptic molecules such as synaptophysin (SYP) (Figure 1F; Figure S1G). We also confirmed the axonal localization of Cdh7 in vitro. As shown in Figure 1G, Cdh7 accumulated in the SYP-containing axon terminal of PN neurons that were cocultured with granule neurons. Together, these results indicate that Cdh7 is selectively expressed in mossy fiber neurons, including PN neurons, and localizes in axon terminals during the synaptogenic stage.

Cdh7 Is Expressed on the Surface of Granule Neurons

Because Cdh7 exhibits homophilic binding, a feature of classic type II cadherins (Dufour et al., 1999; Hirano and Takeichi, 2012), we also examined the expression of Cdh7 in the cerebellum. *Cdh7* mRNA was expressed in the IGL and Purkinje cell layer (PCL) at P12, as well as in the cultured granule neurons (Figures S2A and S2B). We then investigated the expression and localization of Cdh7 protein in the cerebellum. Consistent with the mRNA expression, Cdh7 protein was highly expressed in the IGL and PCL in P14 cerebellum (Figure 2A). In the PCL, Cdh7 was expressed in Purkinje cells with a restricted localization pattern in the cytoplasm but was almost absent from the plasma membrane (Figure 2B). Detailed observations of the cellular distribution of Cdh7 in Purkinje cells revealed that Cdh7 was almost completely confined to the perinuclear structures and was scarcely observed in other cytoplasmic regions (Figure S2C). In the IGL at P14, Cdh7 was expressed in granule neurons and accumulated in their perinuclear structures in the small cytoplasm (Figure 2C). To examine the dendritic localization of Cdh7, we cultured cerebellar neurons. In granule neurons, Cdh7 was clearly localized in the dendrites and accumulated in

(F) A single PN axon terminal in P14 IGL. (Refer to Figure S1G for the low-magnification image.) GFP was expressed in PN axons by in utero electroporation. Section was immunostained with antibodies against Cdh7, SYP and GFP. Note that Cdh7 localizes in the rosette structure of the PN axon terminal (dotted line). (G) Immunostaining for Cdh7, SYP and GFP in PN neurons cocultured with granule neurons for 12 days. PN neurons were visualized by the transfected GFP. Note that Cdh7 localizes in a SYP-containing PN axon terminal (arrow). Scale bars represent 200 μm (D) and 5 μm (F and G).
See also Figure S1 and Table S1.

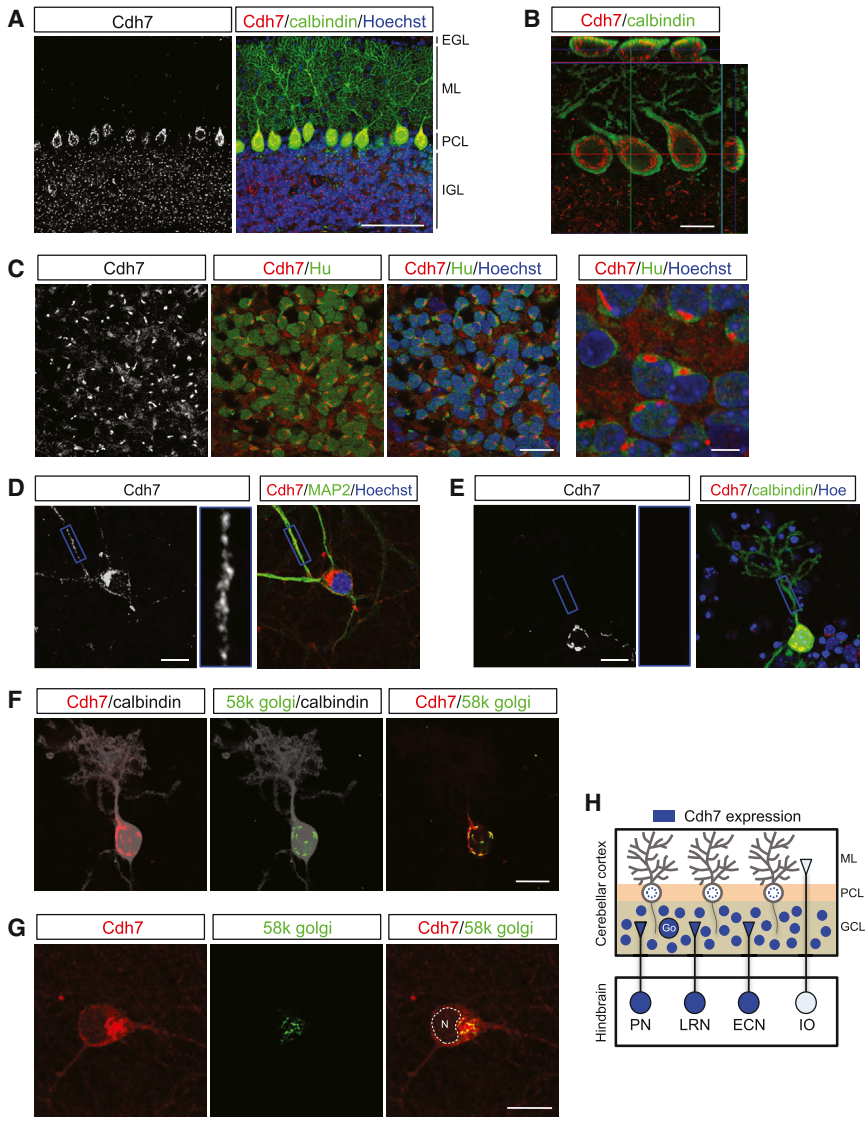

Figure 2. Differential Localization of Cdh7 in Cerebellar Neurons

(A–C) Sections of P14 cerebellum. (A) Immunohistochemistry for Cdh7 and calbindin (a Purkinje cell marker). (B) 3D digital image of Purkinje cells immunostained with antibodies against Cdh7 and calbindin. (C) Granule neurons in the IGL immunostained with antibodies against Cdh7 and Hu.

(D) Immunostaining for Cdh7 and MAP2 (a dendrite marker) in granule neurons at 9 DIV. The blue box indicates a dendrite.

(E and F) Immunostaining for Cdh7, calbindin, and 58k Golgi protein (a Golgi apparatus marker) in 21 DIV Purkinje cells. The blue box in (E) indicates a dendrite. Hoe, Hoechst.

(G) Immunostaining for Cdh7 and 58k Golgi protein in 6 DIV granule neurons. "N" indicates the position of the nucleus.

(H) A summary of Cdh7 expression in the hindbrain and cerebellum. The small blue circles and white circles indicate granule neurons and Purkinje cells, respectively. "Go" indicates a Golgi cell.

Scale bars represent 200 μm (A), 20 μm (B), 20 μm (C, left), 5 μm (C, right), 10 μm (D), 20 μm (E), 20 μm (F), and 10 μm (G). See also Figure S2.

the perinuclear structures (Figure 2D). The dendritic localization of Cdh7 in granule neurons was also observed in vivo (Figures S2D and S2E). In contrast, Cdh7 was detected in neither the dendrites nor the plasma membranes in cultured Purkinje cells, as observed in vivo (Figure 2E). The Cdh7-accumulating perinuclear structures in the granule neurons and Purkinje cells were likely to be the Golgi apparatuses based on the predominant colocalization of Cdh7 and marker proteins for the Golgi apparatus in those structures both in vitro and in vivo (Figures 2F and 2G; Figure S2F). Cdh7 was also expressed in Golgi cells, another target cell for mossy fiber neurons in the IGL, and was localized not only in the Golgi apparatuses but also other cytoplasmic regions (Figures S2F and S2G). The shRNA-mediated knockdown of Cdh7 confirmed the staining for Cdh7; the immunosignals for Cdh7 in cultured Purkinje cells and granule neurons disappeared with the expression of shCdh7 (Figures S2H–S2J). In addition, exogenously expressed Cdh7 was distributed similarly, if not identically, to endogenous Cdh7 in cerebellar neurons, and it was localized at the surface of the dendrites of granule neurons, but not Purkinje cells (Figures S2K–S2P). The subcellular fractionation analyses revealed that endogenous Cdh7 localized in the membranes of granule neurons as well as PN neurons in vitro (Figures S2Q and S2R) and in the synaptosome of P14 IGL, where PN axons and granule neurons form synapses (Figures S2S and S2T). We also analyzed the expression of Cdh7 during cerebellar development. At P9, in addition to the PCL and IGL, Cdh7 was expressed in the outer EGL, whereas Cdh7 expression was low in the inner EGL and ML, suggesting that Cdh7 in granule cells is transiently downregulated during terminal differentiation and migration (Figure S2U). At P23, Cdh7 was expressed in the PCL and IGL, as was also observed at P14 (data not shown).

In summary, during the synaptogenic stage of mossy fiber neurons, Cdh7 is expressed in granule neurons and Golgi cells, which are the target cells for mossy fiber neurons in the IGL, and localized at the surface of the dendrites of granule neurons (Figure 2H). Although Cdh7 is also expressed in Purkinje cells, it is largely confined to the Golgi apparatus, as with cadherin-5 in the pathologic endothelial cells (Groten et al., 2000), and may not be abundantly localized at the cell surface. These results support the hypothesis that Cdh7 mediates the specific connection between PN axons and granule neurons.

Cdh7 Inhibits Axonal Growth in PN Neurons

Because a signal from an ultimate target cell may eventually terminate the growth of innervating axons, we next examined

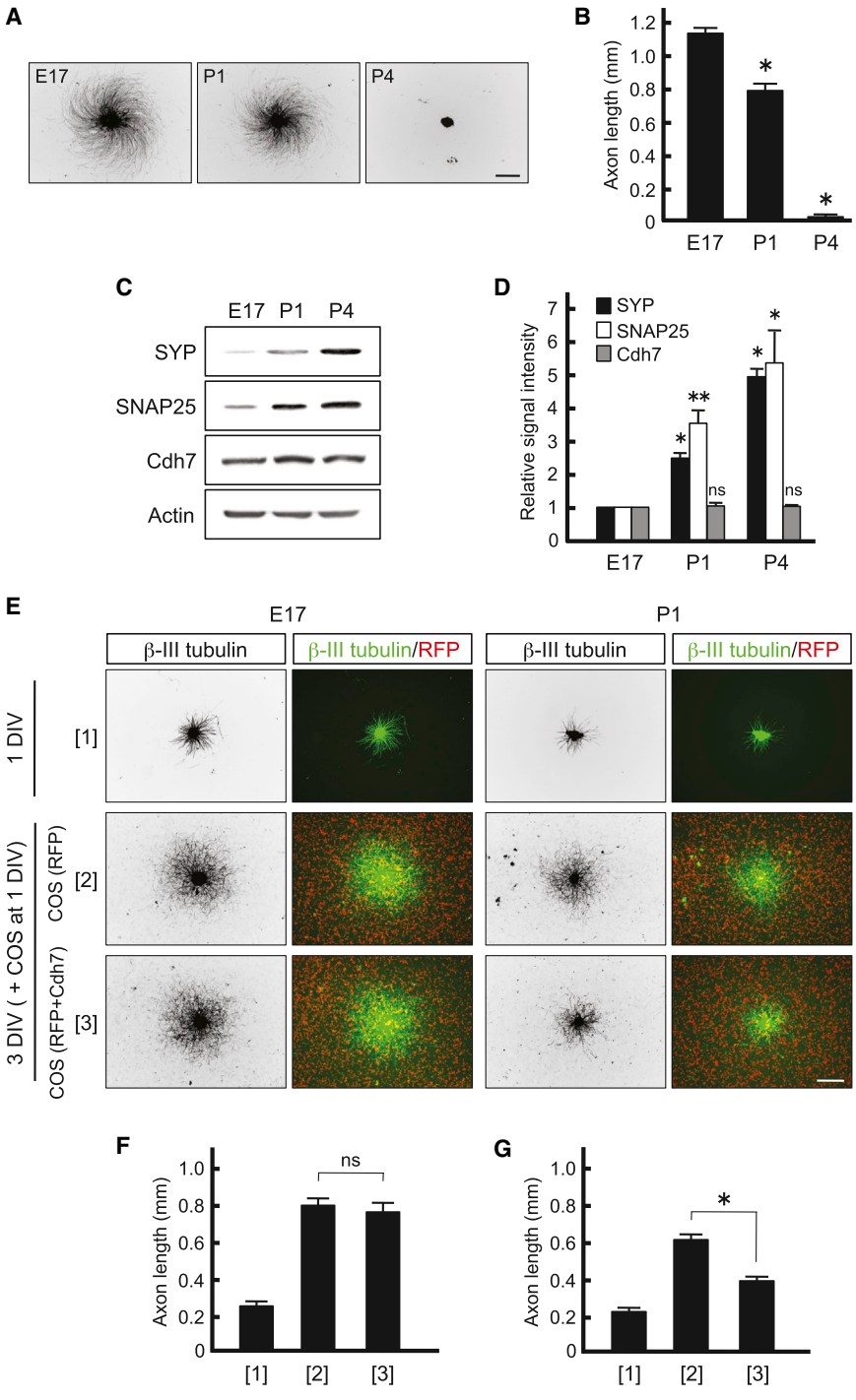

Figure 3. Cdh7 Presented by Surrounding Cells Inhibits PN Axonal Growth in a Stage-Dependent Manner

(A) Axonal growth of PN explants. PN explants from the indicated stages of mice were cultured for 3 days on culture plates coated with poly-D-lysine (PDL) and laminin and immunostained with an antibody against β-III tubulin.

(B) Quantification of the axon length shown in (A). The data represent the mean ± SEM. In total, 47–59 explants were analyzed from three independent experiments. *$p < 0.01$, E17 versus P1 or P4, P1 versus P4.

(C) Western blot analysis of presynaptic molecules in PN neurons in vivo.

(D) Quantification of western blot shown in (C). The signal intensities of SYP, SNAP25, and Cdh7 were normalized to that of actin, and the normalized value for E17 was set at 1.0. The data represent the mean ± SEM of three mice. *$p < 0.01$; **$p < 0.05$; ns, not significant; E17 versus P1 or P4 for each molecule.

(E) PN axonal growth on Cdh7-expressing COS cells. E17 and P1 PN explants were cultured on culture plates coated with PDL and laminin for 1 day. Then, some PN explants were fixed, and control COS cells or Myc-Cdh7-expressing COS cells were added to the others, followed by an additional 2 days culture. The cells were immunostained with an antibody against β-III tubulin. Red fluorescent protein (RFP) was expressed in COS cells.

(F and G) Quantification of the axon length of E17 (F) and P1 (G) PN explants shown in (E). [1], 1 DIV; [2], 3 DIV with control COS cells; [3], 3 DIV with Myc-Cdh7-COS cells. In total, 45–55 explants per condition were analyzed from three independent experiments. The data represent the mean ± SEM. *$p < 0.01$, ns: not significant.

Scale bars in (A) and (E) represent 0.5 mm.

whether Cdh7, which is expressed in both PN axons and granule neurons (Figures 1 and 2), is involved in the termination of axonal growth in PN neurons in the IGL. Consistent with the timing of the arrival of PN axons at the cerebellar cortex, the axonal growth ability of PN neurons was dramatically decreased from E17 to P4 (Figures 3A and 3B), which is consistent with the previous finding that the expression levels of genes associated with axonal growth are downregulated in PN neurons beginning at the first postnatal week (Díaz et al., 2002). Conversely, the expression of synaptic molecules, such as SYP and synaptosomal-associated protein 25 (SNAP25), in PN neurons was highly upregulated from E17 to P4 (Figures 3C and 3D), whereas Cdh7 was expressed at a constant level during this period. These results indicate that developing PN neurons initiate a transition from an "axonal growth phase" to a "synaptogenesis phase" during perinatal development. We first analyzed the effect of Cdh7 presented by surrounding cells on the axonal growth of PN explants at two different developmental stages. To mimic normal development, we first cultured PN neurons alone for 1 day; then, we added control COS cells or Myc-Cdh7-expressing COS cells. E17 PN neurons, which were still in the axonal growth phase, continued to show axonal growth after the addition of COS cells, and Myc-Cdh7-expressing COS cells did not show a difference in the axonal

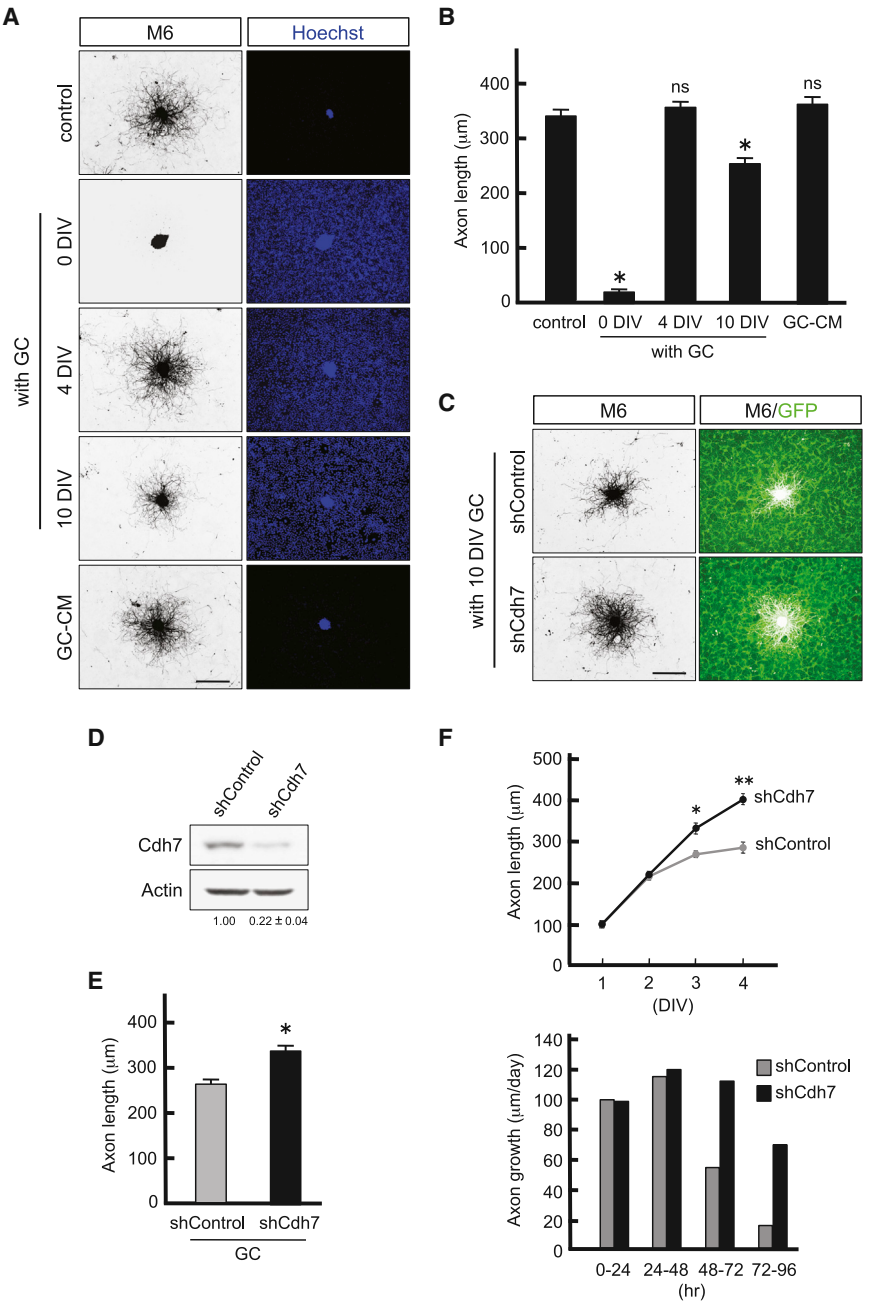

Figure 4. Mature Granule Neurons Diminish the Axonal Growth Potential of PN Neurons through Cdh7

(A) Axonal growth of PN neurons in the coculture with granule cells (GC). Mouse P1 PN explants were added to rat P5 granule cells, which had been precultured for the indicated periods, and were then cocultured for 3 days. Some PN explants were cultured without granule cells (indicated as "control") or in conditioned medium from 10 DIV granule cells (indicated as "GC-CM") for 3 days. Cells were immunostained with an antibody against mouse M6. All cells were cultured on culture plates coated with PDL alone.

(B) Quantification of the axon length of PN neurons shown in (A). In total, 42–70 explants per condition were analyzed from three independent experiments. The data represent the mean ± SEM. *$p < 0.01$; ns, not significant; control versus 0 DIV, 4 DIV, 10 DIV, or GC-CM.

(C) Axonal growth of PN explants cocultured with granule neurons expressing shRNA. Rat P5 granule cells were transfected with expression vectors for shControl or shCdh7 (shCdh7-3), which also encode GFP, and cultured for 10 days. Then, mouse P1 PN explants were added to the 10 DIV granule cells and cocultured for 3 days. Cells were immunostained with an antibody against mouse M6.

(D) Western blot analysis of Cdh7 in shRNA-expressing 10 DIV granule cells in (C). The signal intensities of Cdh7 were normalized to that of actin, and the normalized value of shControl was set at 1.0. The data represent the mean ± SEM of three independent experiments.

(E) Quantification of the axon length of PN neurons shown in (C). In total, 74 PN explants for the shControl group and 62 PN explants for the shCdh7 group were analyzed from three independent experiments. The data represent the mean ± SEM. *$p < 0.05$.

(F) A time course of axonal growth of PN neurons cocultured with granule neurons expressing shRNA. Under the same conditions as in (C), PN explants were cocultured for 1–4 days. The axon length of PN neurons at each time point (top graph) and axonal growth per day (bottom graph) are presented. In total, 58–97 explants per condition were analyzed from three independent experiments. The data represent the mean ± SEM. *$p < 0.05$, **$p < 0.01$, shControl versus shCdh7 at 3 or 4 DIV.

Scale bars represent 300 μm (A and C). See also Figure S3.

growth of PN neurons compared with control COS cells (Figures 3E and 3F). In contrast, the axonal growth of P1 PN neurons, which were presumably transitioning from axonal growth to synaptogenesis, was significantly suppressed by Myc-Cdh7-expressing COS cells (Figures 3E and 3G). These results indicate that the axonal growth of PN neurons may be inhibited by Cdh7 in the surrounding cells, specifically after PN axons have arrived at the cerebellum.

We next investigated whether mature granule neurons inhibit PN axonal growth. We cocultured P1 PN explants with granule cells of different developmental stages. As previously reported (Manzini et al., 2006), 0 days in vitro (DIV) granule cells, which correspond to "EGL-like" immature granule cells, strongly inhibited PN axonal growth, whereas 4 DIV granule neurons did not show this effect (Figures 4A and 4B). In comparison, 10 DIV "IGL-like" mature granule neurons, which expressed much higher levels of Cdh7 than immature granule cells (Figure S3A) and possessed much longer and arborized dendrites than 4 DIV granule neurons (Figure S3B), also significantly suppressed the axonal growth of PN neurons, though this suppression was less effective than that of 0 DIV granule cells (Figures 4A and 4B). Conditioned medium from 10 DIV granule neurons did not

suppress the axonal growth of PN neurons, suggesting that secreted molecules may not exert this effect (Figures 4A and 4B). Next, we tested the possibility that Cdh7 mediates the suppression of PN axonal growth by mature granule neurons. P1 PN explants were cocultured with shRNA-expressing 10 DIV granule neurons (Figures 4C and 4D). After 3 days culture, the axon length of PN neurons cultured with shControl-expressing granule neurons (269.0 ± 7.1 μm; Figure 4E) was almost identical to that of PN neurons cultured with nontransfected 10 DIV granule neurons (257.8 ± 8.1 μm; Figure 4B). Axon length in PN neurons was significantly increased by coculture with shCdh7-expressing granule neurons in comparison to coculture with shControl-expressing granule neurons (Figure 4E), and Cdh7 knockdown largely blocked the suppressive effect of 10 DIV granule neurons on the axonal growth of PN neurons (346.0 ± 10.4 μm, "control" in Figure 4B versus 332.4 ± 7.2 μm, "shCdh7" in Figure 4E; $p > 0.05$). These results suggest that mature granule neurons in the IGL inhibit the axonal growth of PN neurons through Cdh7. We further analyzed the time course of the growth rate of PN axons on 10 DIV granule neurons (Figure 4F). During the first 2 days in coculture with shControl-expressing granule neurons, the growth rates of PN axons were 99.6 μm per day for 0–24 hr and 115.6 μm per day for 24–48 hr. Thereafter, the growth rate dropped greatly to 16.1 μm per day for 72–96 hr, and this decrease in axonal growth was significantly inhibited by coculture with shCdh7-expressing granule neurons (Figure 4F). These results indicate that, through a mechanism that reduces the axonal growth rate, Cdh7 may be involved in the program that terminates PN axonal growth in the IGL.

Cdh7 Mediates Specific Connections in the Pontocerebellar Circuit In Vivo

The expression pattern of Cdh7 in the hindbrain and cerebellum prompted us to explore whether Cdh7 regulates the connectivity of mossy fiber axons. We investigated the importance of Cdh7 in the specific circuit formation of PN neurons in vivo by shRNA-mediated knockdown with an in utero electroporation method (Figures S4A–S4D). We found that shCdh7-expressing PN neurons developed normally, forming the PN and projecting axons to the cerebellum (Figures S4B and S4C). To examine the target specificity of PN axons in the cerebellum, we analyzed the contact of PN axons with nontarget Purkinje cells, which is transiently observed in some PN axons during development (Mason and Gregory, 1984). Very detailed light and electron microscopy analyses previously revealed that the transient contacts between mossy fibers and Purkinje cells at P7 exhibit ultrastructural characteristics of synapses and that after P7, those synaptic contacts are dramatically decreased and eventually disappear by P21 (Kalinovsky et al., 2011). To assess the effect of Cdh7 knockdown on the connectivity of PN axons, we first analyzed PN axons in P14 cerebellum. In the shControl group, the majority of PN axons terminated in the IGL, and only a few PN axons contacted the Purkinje cells and invaded the ML (Figure 5A). However, in one of the shCdh7 groups (shCdh7-2), the numbers of Purkinje cells that received PN axon contacts and PN axons that invaded the ML were increased 11.7-fold and 3.4-fold, respectively, compared with the shControl group (Figures 5A–5C). The coexpression of shCdh7-2-resistant Cdh7, with silent mutations insensitive to shCdh7-2, largely reversed the defects caused by shCdh7-2 (Figures 5A–5C; Figure S2H). Furthermore, the expression of the other shCdh7 (shCdh7-1) also increased the numbers of PN axon-contacted Purkinje cells and PN axons in the ML to a degree similar to that observed in the shCdh7-2 group (Figures 5A–5C). To estimate the percentage of Purkinje cells receiving PN axon contacts, we analyzed mice in which a large number of PN axons expressed shRNAs in the IGL. Under these conditions, 76.4% of the Purkinje cells received PN axon contacts in the shCdh7 group, whereas only 7.1% received PN axon contacts in the shControl group (Figure S4E). Similar patterns of PN axon contacts with Purkinje cells were observed in mice in which a small number of PN axons expressed each shRNA (Figure S4F). We also found that the positions of the rosette structures of the PN axons in the IGL were significantly shifted toward the PCL in the shCdh7 group (Figure S4G). Furthermore, unlike the shControl-expressing PN axons, which mainly contacted Purkinje cells at the bottom half of the cell body, shCdh7-expressing PN axons contacted Purkinje cells at more upper regions, including the dendrites (Figure S4H). Together, these results indicate that the loss of Cdh7 in PN neurons impairs the connectivity of PN axons in the cerebellum.

We also analyzed the connectivity of PN axons at other developmental stages. Consistent with previous study (Kalinovsky et al., 2011), in the shControl group, many more Purkinje cells received PN axon contacts at P7 compared with P14, and those contacts had mostly disappeared by P21 (Figures 5D and 5E). The number of Purkinje cells receiving PN axon contacts was significantly increased in the shCdh7 group as early as P7, when granule neurons begin to migrate into the IGL region (Figures 5D and 5E), suggesting that the contact between PN axons and Purkinje cells in the shCdh7 group is already augmented prior to the onset of the elimination of PN axons from Purkinje cells. Then, along with the dramatically increased number of granule neurons that migrate into the IGL, the difference between the shControl and shCdh7 groups in the number of Purkinje cells receiving PN axon contacts was highly expanded at P14 (Figure 5E). There was still a significant difference in the number of PN axon-Purkinje cell contacts between the shControl and shCdh7 groups at P21 (Figures 5D and 5E), even though Purkinje cells receiving PN axon contacts in the shCdh7 group was decreased compared with P14. These results suggest that the augmented contact between PN axons and Purkinje cells in the shCdh7 group might be attributed to the impairment in the mechanism selectively connecting PN axons to granule neurons rather than to a defect in the elimination of PN axons.

shControl-expressing PN axon terminals in the IGL at P14 exhibited the characteristic rosette structures containing SYP (Figure 5F; Figure S4I). However, in the shCdh7 group, we occasionally observed presumptive PN axon terminals showing structures that were slightly swollen but much smaller than normal rosettes (Figure 5F). Although we still observed many rosettes of normal shape and size in shCdh7-expressing PN axons, the number of SYP-containing rosettes in the IGL that were wider than 3 μm was significantly decreased in the shCdh7 group (Figures 5G and 5H), suggesting that the loss of Cdh7 in PN neurons also partially affects the synapse formation of PN axons with granule neurons and Golgi cells in vivo.

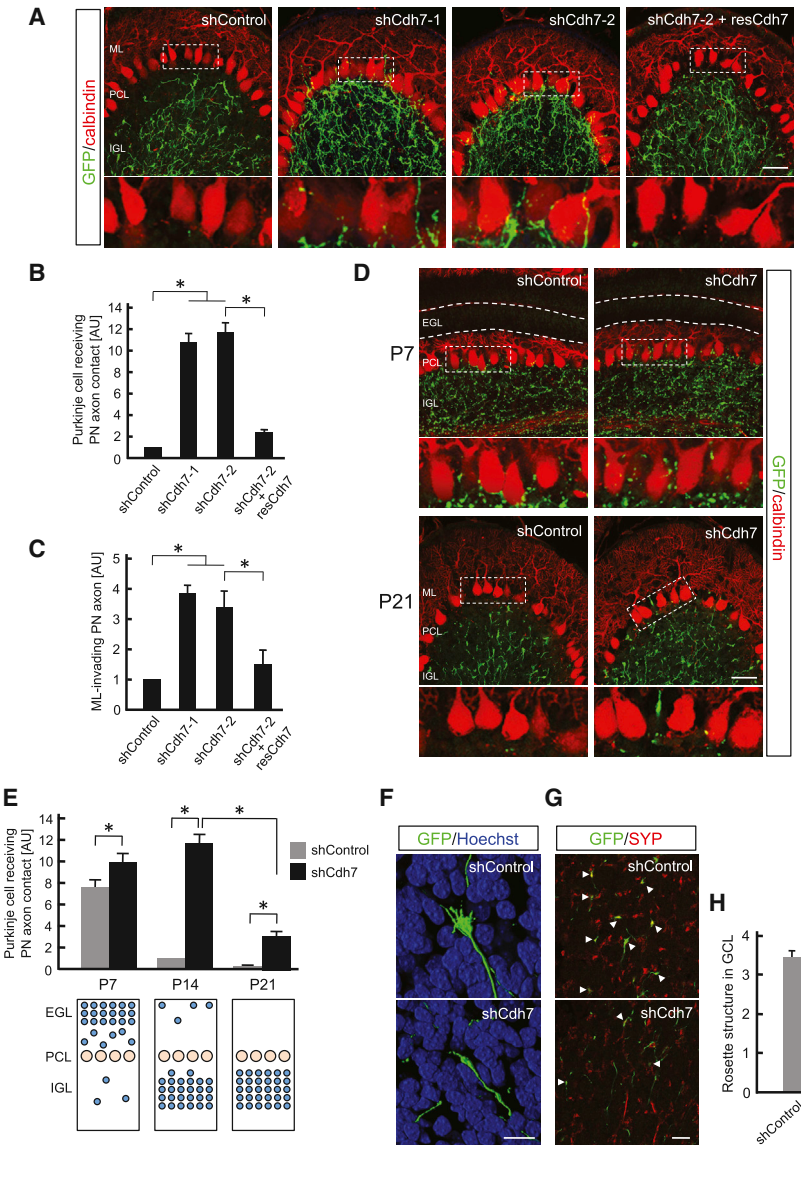

Figure 5. Knockdown of Cdh7 Impairs Connectivity of PN Axons In Vivo

Cerebella of mice expressing shRNAs and cDNA in PN neurons by in utero electroporation. Control shRNA (shControl), shRNAs for Cdh7 (shCdh7-1 and shCdh7-2), and shCdh7-2-resistant Cdh7 (resCdh7) were expressed in PN neurons. The term "shCdh7" specifically means shCdh7-2. PN axons were visualized by the coexpression of GFP.

(A) Sections of P14 cerebellum were immunostained with antibodies against GFP and calbindin. The dotted boxes indicate the positions of the high-magnification images shown in the bottom panels.

(B and C) Quantification of the Purkinje cells that received PN axon contacts (B) and PN axons that invaded the ML (C) shown in (A). The numbers of Purkinje cells and PN axons were normalized to the occupancy of GFP-positive PN axons in the IGL, and the normalized value of shControl was set at 1.0. Data are presented as the mean ± SEM (arbitrary units [AU]). In total, six to eight mice per condition were analyzed. *$p < 0.01$.

(D) Sections of P7 and P21 cerebella of mice expressing shRNAs in PN neurons. Sections were immunostained with antibodies against GFP and calbindin. The boxes indicate the positions of the high-magnification images shown in the bottom panels.

(E) Quantification of the Purkinje cells that received PN axon contacts. The number of Purkinje cells was normalized as in (B) and (C), and the normalized value for shControl at P14 was set at 1.0. The data are presented as the mean ± SEM (AU). *$p < 0.01$. In total, six to eight mice per condition were analyzed. The scheme indicates the position of granule cells (blue circles) at each stage.

(F–H) Cerebella of P14 mice expressing shRNAs in PN neurons. Sections were immunostained with antibodies against GFP and SYP. (F) Morphology of PN axon terminals in the IGL. Note that the abnormal structure of the presumptive PN axon terminal was observed in the shCdh7 group. (G) Low-magnification images of the IGL region. The arrowheads indicate the rosette of a PN axon terminal in the IGL. (H) Quantification of the SYP-containing rosette greater than 3 μm in width in the IGL. The number of rosettes was normalized as in (B) and (C), and the value is presented as the mean ± SEM per 100 μm^2 GFP-positive PN axon area in the IGL. Four mice from each group were analyzed. *$p < 0.01$.

Scale bars represent 50 μm (A and D), 10 μm (F), and 20 μm (G). See also Figure S4.

Cdh7 Mediates Synapse Formation between PN Neurons and Granule Neurons

To test the possibility that the abnormal connectivity of shCdh7-expressing PN axons in vivo is due to a defect of specific synapse formation between PN axons and granule neurons, we next examined the role of Cdh7 in synapse development in cocultured PN neurons and granule neurons (Figures 6A–6C). Closely apposed SYP-positive presynaptic and postsynaptic density 95 (PSD95)-positive postsynaptic puncta on shRNA-expressing PN axons indicated mature synapses. As shown in Figures 6A and 6B, the knockdown of Cdh7 in PN neurons significantly decreased the number of synapses, suggesting that Cdh7 promotes synapse development between PN neurons and granule neurons. In contrast, when PN neurons were cocultured with nontarget Purkinje cells, the number of SYP-containing PN axons that contacted Purkinje cells was not altered by the knockdown of Cdh7 in PN neurons (Figures 6D and 6E), supporting the confined cytoplasmic localization of Cdh7 in Purkinje cells (Figure 2). Together, these results suggest that Cdh7 is selectively required for synapse development between PN axons and granule neurons.

Because the total number of SYP puncta in the PN axons cocultured with granule neurons was significantly reduced in the shCdh7 group compared with the shControl group (Figure 6C), we next examined whether Cdh7 was involved in the induction of presynaptic differentiation in PN axons. When cocultured

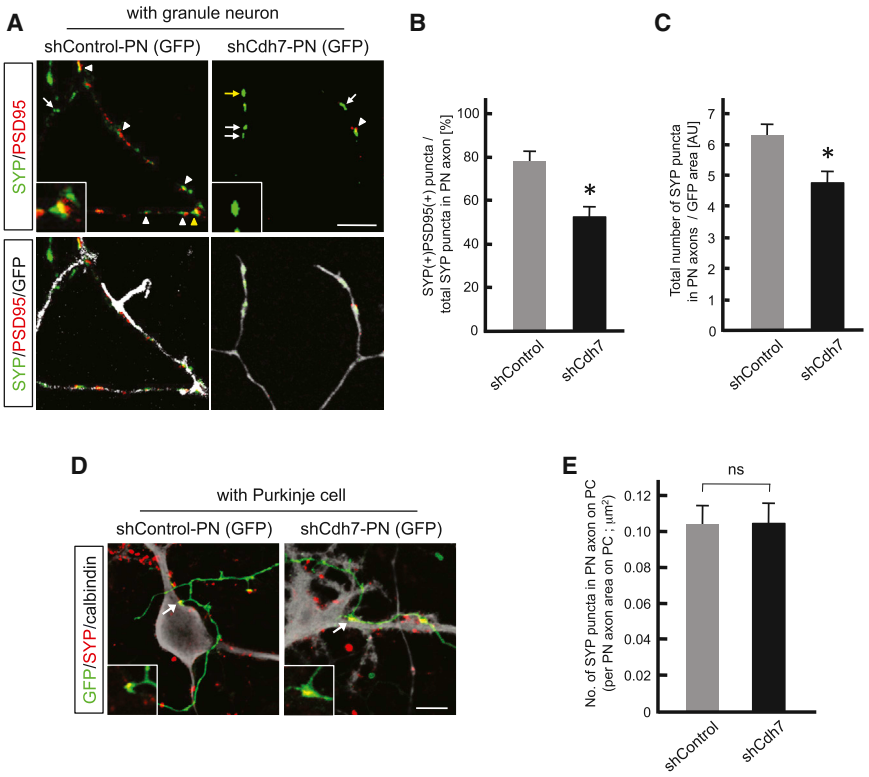

Figure 6. Cdh7 Mediates Synapse Formation between PN Neurons and Granule Neurons

(A) shRNA-expressing PN neurons were cocultured with granule neurons for 12 days. Cells were immunostained with antibodies against GFP, SYP, and PSD95. PN axons were visualized by GFP, which is presented in white pseudocolor. The arrowheads indicate SYP puncta that are closely apposed with postsynaptic PSD95 puncta. The arrows indicate PSD95-free SYP puncta. The yellow arrow and arrowhead indicate the magnified puncta (insets).

(B and C) Quantification of SYP puncta shown in (A). (B) The percentage of SYP puncta closely apposed with PSD95 puncta among all SYP puncta in PN axons. The data represent the mean ± SEM. *$p < 0.01$. (C) The total number of SYP puncta in PN axons, normalized to the area of the PN axons. The data represent the mean ± SEM (AU). *$p < 0.05$. In total, 52 fields for the shControl group and 57 fields for the shCdh7 group were analyzed from three independent experiments.

(D) shRNA-expressing PN neurons were added to 10 DIV Purkinje cells. Neurons were cocultured for 11 days and immunostained with antibodies against GFP, SYP, and calbindin. PN axons were visualized by GFP. The arrows indicate the magnified puncta (insets).

(E) The number of SYP puncta in PN axons in contact with Purkinje cells, which is normalized to the area of the PN axons associated with Purkinje cells shown in (D). In total, 63 fields for the shControl group and 62 fields for the shCdh7 group from four independent experiments were analyzed. The data represent mean ± SEM ns: not significant. Scale bars represent 5 μm (A) and 10 μm (D).

with COS cells, Myc-Cdh7 presented by COS cells strongly induced the clustering of the presynaptic component SYP in PN axons, but not in IO axons, whereas protocadherin-20 (Pcdh20), which is not expressed by PN neurons, had no effect (Figures 7A and 7C; Figures S5A–S5D). In the coculture of PN neurons and COS cells expressing Myc-Cdh7, SYP was clustered in the segments of PN axons that contacted the accumulated puncta of Myc-Cdh7 in COS cells (Figure S5E). Myc-Cdh7-induced SYP clustering in PN axons was largely inhibited by the knockdown of Cdh7 in PN neurons (Figures 7B and 7D). These results indicate that the Cdh7-Cdh7 interaction may induce presynaptic differentiation specifically in PN neurons.

DISCUSSION

A Transition from Axonal Outgrowth to Synapse Formation

Axonal outgrowth, pathfinding, and synaptogenesis are tightly interlinked steps during neural circuit formation. A spatiotemporally coordinated transition from axonal growth to synaptogenesis is essential for establishing precise synaptic connectivity in the nervous system. Previous studies have identified molecules that are involved in the development of both axons and synapses. The conserved PHR family of E3 ubiquitin ligases regulates axon guidance, growth, and synapse formation (Po et al., 2010). The serine/threonine kinase SAD-1 regulates axonal growth termination and presynaptic differentiation in *Caenorhabditis elegans* (Crump et al., 2001). S-laminin, which is a basal lamina protein of the muscle, mediates selective reconnection of regenerating motor axons to the original synaptic "trace" on denervated muscle fibers and inhibits the axonal growth of motor neurons (Porter et al., 1995). However, a mechanism that directly orchestrates synaptic connection and axonal growth termination during neural development has not yet been elucidated.

Synaptogenesis consists of multiple steps, including nascent synaptic contacts between axons and dendrites, selection of bona fide synapses, and maturation of synapses (Waites et al., 2005; Jontes and Phillips, 2006). Increasing evidence indicates that nascent nonspecific contacts between axons and dendrites are continuously formed and eliminated during the early stage of synaptogenesis (Niell et al., 2004; Li et al., 2011). Thus, at this stage, the axons retain motility and are not yet stabilized in their target regions. During this period, target cell-derived signals may prime the innervating axons to undergo synaptogenesis (Waites et al., 2005). Thereafter, some contacts are selectively stabilized to form bona fide synapses, and growing axons terminate their growth at this stage. A specific set of synaptic adhesion molecules that directly mediates axon-target connections may selectively promote strong adhesion between pre- and postsynaptic membranes of the appropriate cells, thereby establishing synaptic specificity (Waites et al., 2005; Jontes and Phillips, 2006). The cadherin superfamily has been the main candidate for regulating synaptic

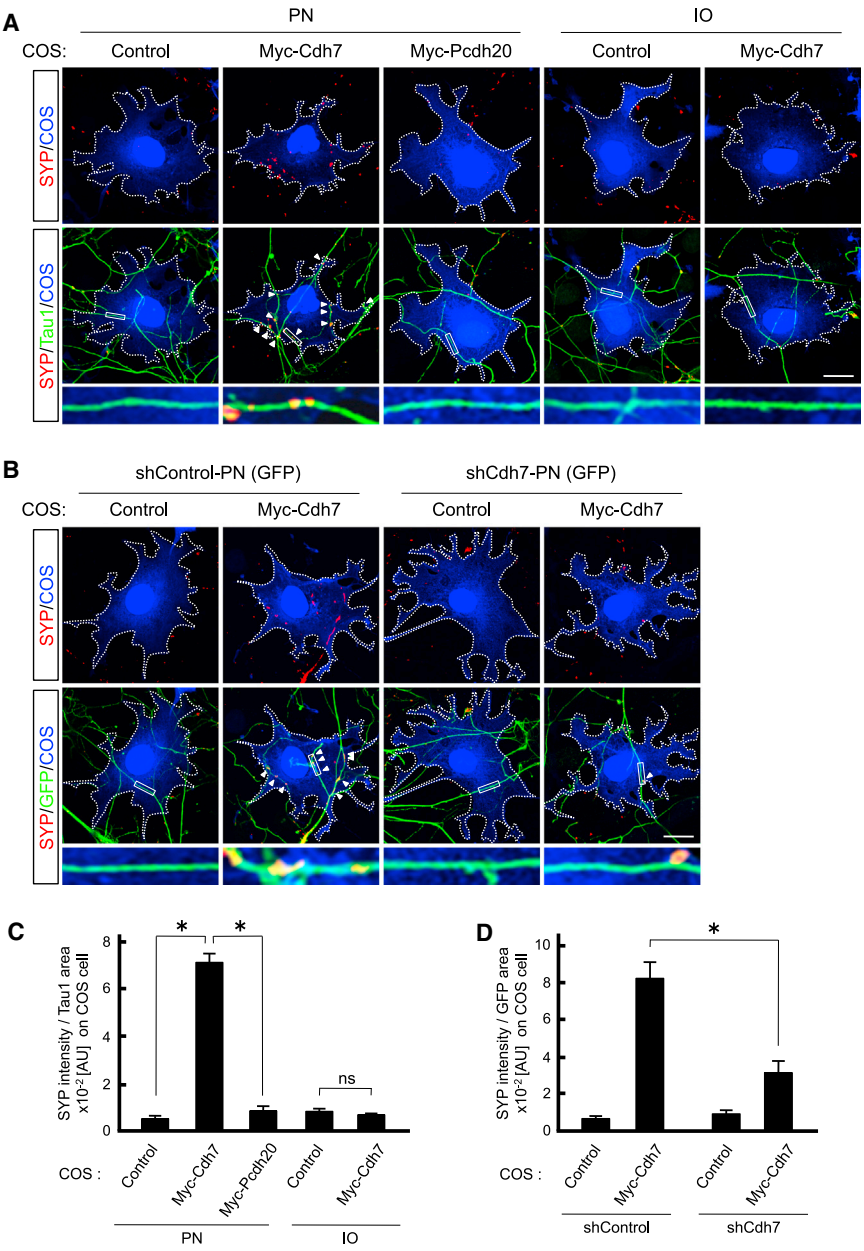

Figure 7. Cdh7-Cdh7 Signaling Induces Presynaptic Differentiation in PN Axons

(A) PN and IO neurons were cultured for 7 days; then, control COS cells or Myc-Cdh7/Myc-Pcdh20-expressing COS cells were added and cocultured for 1 day. Cells were immunostained with antibodies against SYP and Tau1 (an axon marker). RFP was expressed in COS cells to visualize the entire cell. RFP fluorescence is presented in blue pseudocolor and indicated as "COS." A single COS cell is surrounded by a dotted line. The arrowheads indicate the clusters of SYP in Tau1-positive axons associated with the COS cell. The boxes indicate the positions of the high-magnification images shown in the bottom panels.

(B) PN neurons were transfected with expression vectors for shRNAs and cultured for 7 days; then, control COS cells or Myc-Cdh7-expressing COS cells were added and cocultured for 1 day. Cells were immunostained with antibodies against SYP and GFP. PN axons were visualized by GFP, which was encoded by the shRNA vector. The entire COS cell was visualized by RFP and is presented in blue pseudocolor, as noted in (A). The arrowheads indicate the clusters of SYP in PN axons associated with the COS cell. The boxes indicate the positions of the high-magnification images shown in the bottom panels.

(C and D) Quantification of the total integrated intensity of SYP associated with a single COS cell divided by the Tau1-positive (C) or GFP-positive (D) axon contact area, shown in (A) and (B), respectively. In total, 30–32 COS cells per condition from three to four independent experiments were analyzed. The data represent the mean ± SEM (AU). *$p < 0.01$; ns, not significant.

Scale bars represent 20 μm (A and B). See also Figure S5.

specificity because of its large molecular diversity and circuit-specific expression patterns (Takeichi, 2007), even though only a few members have been demonstrated to regulate synaptic specificity, particularly in mammals (Osterhout et al., 2011; Williams et al., 2011). Cdh7 is expressed at the surface of PN neurons and granule neurons (Figures 1 and 2; Figures S1 and S2) and specifically mediates synapse formation between those neurons (Figure 6); thus, after the granule neuron-derived synaptogenic priming molecules, such as Wnt7a and FGF22 (Hall et al., 2000; Umemori et al., 2004), make PN axons competent to proceed with synaptogenesis (Waites et al., 2005), the Cdh7-Cdh7 interaction may selectively stabilize nascent contacts between PN axons and granule neurons to develop bona fide synapses. Cadherin-mediated synaptic contacts can trigger synaptic differentiation through the recruitment of various synaptic proteins to the contact site, including presynaptic organizers, scaffold proteins, and signaling molecules (Hirano and Takeichi, 2012). Therefore, the Cdh7-mediated selective contacts between PN axons and granule neurons may strongly promote synaptic differentiation in those neurons by accumulating synaptic inducers, such as neuroligin (Scheiffele et al., 2000), to the synaptic contact site. Because Cdh7 per se can induce the clustering of SYP in PN axons (Figure 7), which is consistent with the previous finding that classic cadherins induce presynaptic differentiation during the early stage of synaptogenesis in hippocampal neurons (Togashi et al., 2002), Cdh7 may also function as an inducer of synaptic differentiation in this circuit.

The present study elucidated another function of Cdh7 during the development of the pontocerebellar circuit. Because Cdh7 presented by mature granule neurons diminishes the growth potential of PN axons (Figure 4), the Cdh7-Cdh7 interaction between PN neurons and granule neurons may also function to

suppress the motility of PN axons, presumably to terminate axonal movement and form bona fide synapses in the IGL. Several cadherin superfamily members positively or negatively regulate neurite outgrowth depending on cell type and developmental stage (Fredette et al., 1996; Riehl et al., 1996; Siu et al., 2007). Given that a mechanical association of N-cadherin and cytoskeletal proteins via catenins at the intracellular domain critically regulates neurite outgrowth and growth cone motility (Bard et al., 2008), the Cdh7-Cdh7 interaction may directly signal to reduce the motility of PN axons through cytoskeletal remodeling. Alternatively, Cdh7 may indirectly inhibit the axonal growth of PN neurons by recruiting other axonal growth inhibitors to the synaptic contact site. Further studies are anticipated to disclose the molecular mechanism of the Cdh7-mediated regulation of axonal growth potential.

Cdh7 may link the two sequential steps, axonal growth and synaptogenesis, during the development of the pontocerebellar circuit through the regulation of axonal growth potential and axon-target connection. This coupled mechanism, exerted by a single cell-surface receptor, may allow developing neurons to promptly and properly transit from axonal growth to synaptogenesis without unfavorable errors, such as axon overshooting or underdevelopment of synapses, which would likely cause defects in the circuit function. It will be interesting to examine whether other molecules that have been previously demonstrated to mediate synaptic specificity also inhibit axonal growth in each context.

Mechanism for Establishing Specific Connections in the Pontocerebellar Circuit

The recent finding that Purkinje cell-derived BMP4 eliminates the connections between PN axons and Purkinje cells strongly supports the importance of the error-correction-based mechanism for the wiring of the pontocerebellar circuit (Kalinovsky et al., 2011). However, we hypothesize that a target-cell-derived signal that selectively connects PN neurons and granule neurons is likely involved in the formation of the pontocerebellar circuit, based on the following evidence: (1) the vast majority of mossy fibers still terminate in the IGL, even in *BMP4*-deficient mice (Kalinovsky et al., 2011); (2) mossy fibers synapse with abnormally stranded granule neurons in the ML in *Sema6a*-deficient mice (Kerjan et al., 2005); and (3) granule neurons preferentially connect to PN axons versus IO axons in vitro (Ito and Takeichi, 2009). Therefore, we regard the Cdh7-mediated specific connection between PN axons and granule neurons as a key mechanism in establishing the outline of the connectivity of this circuit (Figure S4J).

Based on the present findings, there are various possible mechanisms of the Cdh7-mediated regulation of circuit connectivity. Because PN axons start to contact Purkinje cells before granule neurons migrate into the IGL, granule neurons, which dramatically increase in number in the IGL at later stages, may compete with Purkinje cells for contact with PN axons. Supporting this idea, the contacts between mossy fibers and Purkinje cells persist in the agranular cerebellum of *weaver* mice, in which granule cells die prior to migration (Sotelo, 1975). In addition, this competition mechanism may explain the augmented contacts between shCdh7-expressing PN axons and Purkinje cells in vivo (Figure 5), because PN axons may lose the potential of the preferential synapse formation with granule neurons in the absence of Cdh7 (Figure 6). Furthermore, from P7 to P14, the expanded difference in the number of Purkinje cells that receive PN axon contacts between the shControl and shCdh7 groups (Figure 5E) may be due to the explosively increased number of granule neurons in the IGL during this period, which may accelerate the translocation of PN axons from Purkinje cells to granule neurons in the shControl group. In addition to this model, the present finding that mature granule neurons inhibit the outgrowth of PN axons through Cdh7 (Figure 4) raises another possibility. The Cdh7-Cdh7 interaction between PN neurons and mature granule neurons may confine PN axons to the IGL through a mechanism inhibiting axonal growth, thereby contributing to the specific circuit connectivity. shCdh7-expressing PN axons may not completely restricted to the IGL even in the presence of mature granule neurons because of the loss of the Cdh7-Cdh7 interaction. Similarly, PN axons may not fully stop growing in the IGL in the absence of mature granule neurons in *weaver* mice. In these contexts, PN axons may remain motile even in the middle or late synaptogenic stages, such as P14, and may largely increase nonspecific contacts to Purkinje cells beyond the reach of the BMP4-mediated elimination mechanism. Collectively, it is plausible that the mechanisms of the Cdh7-mediated selective target recognition and axonal growth inhibition may coordinately establish the connectivity of the pontocerebellar circuit.

Axonal Growth Termination of PN Neurons

Because PN axons initially slow down below the EGL, transiently contact Purkinje cells at the PCL and ML and subsequently settle in the IGL to form synapses with granule neurons and Golgi cells, the termination of axonal growth in PN neurons is likely to be regulated in a spatiotemporally stepwise manner. Similar axonal growth termination via transient contact with nontarget cells is observed in other circuits, including the thalamocortical and hippocampal circuits (Ghosh et al., 1990; Del Río et al., 1997). Thus, in the target region, axonal growth may stop in a stepwise manner, at least in some cases. In the pontocerebellar circuit, the EGL-derived signal(s), including a heparin-binding factor-dependent signal, would be a strong candidate for the initial inhibitory signal against growing PN axons that enter the cerebellar cortex (Manzini et al., 2006). Because the axonal growth potential of PN neurons is dramatically downregulated at the perinatal stage (Figures 3A and 3B), when PN axons encounter immature granule cells in the EGL (Ashwell and Zhang, 1992; Manzini et al., 2006), there is a possibility that an EGL-derived stop signal primes PN neurons to halt the axonal growth program, and this may cause the reduced growth potential of PN axons in the IGL at the later stage and contribute to the developmental-stage-dependent differential susceptibility of PN axons to environmental Cdh7 (Figure 3). Because it is reasonable that a signal from the ultimate target cell completely terminates the growth of innervating axons, Cdh7 presented by mature granule neurons may participate in the mechanism terminating PN axonal growth in the IGL. Continued work on the growth potential of PN axons in the cerebellum would facilitate the understanding of the entire mechanism of axonal growth termination.

EXPERIMENTAL PROCEDURES

Animals

All animal care and experimental procedures were performed in accordance with institutional guidelines approved by the Experimental Animal Care Committee of the Keio University School of Medicine (approval number 09091-10). The day of the vaginal plug confirmation was counted as E0, and the day of birth was counted as P0.

Western Blot

The mouse tissues and cultured cells were homogenized with lysis buffer (TNE buffer) containing 10 mM Tris-HCl (pH 8.0), 150 mM NaCl, 1 mM EDTA, 1% Nonidet P-40, and protease inhibitors (Complete, Roche Applied Science) and centrifuged at 12,000 × *g* for 30 min at 4°C to obtain the supernatant. The lysates were separated by 10% SDS-polyacrylamide gel electrophoresis, blotted onto Immobilon membrane (Millipore) and incubated with primary antibodies. After incubation with horseradish peroxidase (HRP)-conjugated antibodies, the proteins were detected by the chemiluminescence method (ECL, GE Healthcare; SuperSignal West Dura Extended Duration Substrate, Thermo Scientific). Signal intensities were measured with an image analyzer (LAS-4000, GE Healthcare) and quantified with Image Quant TL (GE Healthcare).

Immunohistochemistry and Immunocytochemistry

Immunostaining was performed as previously described (Kuwako et al., 2010). Briefly, the tissues were fixed with 4% paraformaldehyde (PFA) in PBS overnight at 4°C. Then, 60-μm-thick tissue sections were prepared using a vibratome (VT1200S, Leica). Cultured cells were fixed with 4% PFA-PBS for 20 min at 4°C. The fixed sections and cells were permeabilized with 0.3% Triton X-100-PBS for 15 min at room temperature (RT), incubated with TNB blocking buffer (PerkinElmer) for 1 hr at RT and subsequently incubated with primary antibodies in TNB blocking buffer overnight at 4°C, followed by incubation with fluorescent-dye-conjugated secondary antibodies for 1.5 hr at RT. Nuclei were counterstained with Hoechst 33258 (10 μg/ml, Sigma-Aldrich). The images were observed by fluorescence microscopy (BZ-9000, Keyence) and confocal laser scanning microscopy (LSM700, Carl Zeiss).

RT-PCR

Total mRNA was extracted from the mouse tissues, cultured neurons, and specific layers of cerebellar tissue prepared by the laser microdissection method using TRIzol Reagent (Life Technologies). After reverse transcription, PCR was conducted using PrimeSTAR Max DNA Polymerase (Takara Bio).

For other procedures, refer to the Supplemental Experimental Procedures.

SUPPLEMENTAL INFORMATION

Supplemental information includes Supplemental Experimental Procedures, five figures, and one table and can be found with this article online at http://dx.doi.org/10.1016/j.celrep.2014.08.063.

ACKNOWLEDGMENTS

We thank the members of the Okano laboratory, especially Dr. S. Suyama, at Keio University for technical advice and helpful discussions. This work was supported by grants from the Japan Society for the Promotion of Science, the Brain Science Foundation, The Kanae Foundation for the Promotion of Medical Science, and the Narishige Neuroscience Research Foundation (to K.K.), and the Funding Program for World-leading Innovative R&D on Science and Technology (to H.O.). H. O. is a Founding Scientist and a paid SAB of San Bio Co., Ltd.

Received: December 31, 2013
Revised: July 18, 2014
Accepted: August 25, 2014
Published: October 2, 2014

REFERENCES

Altman, J., and Bayer, S.A. (1997). Development of the Cerebellar System: In Relation to its Evolution, Structure and Functions (Boca Raton: CRC Press).

Ashwell, K.W., and Zhang, L.L. (1992). Ontogeny of afferents to the fetal rat cerebellum. Acta Anat. (Basel) *145*, 17–23.

Bard, L., Boscher, C., Lambert, M., Mège, R.M., Choquet, D., and Thoumine, O. (2008). A molecular clutch between the actin flow and N-cadherin adhesions drives growth cone migration. J. Neurosci. *28*, 5879–5890.

Crump, J.G., Zhen, M., Jin, Y., and Bargmann, C.I. (2001). The SAD-1 kinase regulates presynaptic vesicle clustering and axon termination. Neuron *29*, 115–129.

Del Río, J.A., Heimrich, B., Borrell, V., Förster, E., Drakew, A., Alcántara, S., Nakajima, K., Miyata, T., Ogawa, M., Mikoshiba, K., et al. (1997). A role for Cajal-Retzius cells and reelin in the development of hippocampal connections. Nature *385*, 70–74.

Díaz, E., Ge, Y., Yang, Y.H., Loh, K.C., Serafini, T.A., Okazaki, Y., Hayashizaki, Y., Speed, T.P., Ngai, J., and Scheiffele, P. (2002). Molecular analysis of gene expression in the developing pontocerebellar projection system. Neuron *36*, 417–434.

Dufour, S., Beauvais-Jouneau, A., Delouvée, A., and Thiery, J.P. (1999). Differential function of N-cadherin and cadherin-7 in the control of embryonic cell motility. J. Cell Biol. *146*, 501–516.

Fredette, B.J., Miller, J., and Ranscht, B. (1996). Inhibition of motor axon growth by T-cadherin substrata. Development *122*, 3163–3171.

Ghosh, A., Antonini, A., McConnell, S.K., and Shatz, C.J. (1990). Requirement for subplate neurons in the formation of thalamocortical connections. Nature *347*, 179–181.

Groten, T., Kreienberg, R., Fialka, I., Huber, L., and Wedlich, D. (2000). Altered subcellular distribution of cadherin-5 in endothelial cells caused by the serum of pre-eclamptic patients. Mol. Hum. Reprod. *6*, 1027–1032.

Hall, A.C., Lucas, F.R., and Salinas, P.C. (2000). Axonal remodeling and synaptic differentiation in the cerebellum is regulated by WNT-7a signaling. Cell *100*, 525–535.

Hirano, S., and Takeichi, M. (2012). Cadherins in brain morphogenesis and wiring. Physiol. Rev. *92*, 597–634.

Ito, S., and Takeichi, M. (2009). Dendrites of cerebellar granule cells correctly recognize their target axons for synaptogenesis in vitro. Proc. Natl. Acad. Sci. USA *106*, 12782–12787.

Jontes, J.D., and Phillips, G.R. (2006). Selective stabilization and synaptic specificity: a new cell-biological model. Trends Neurosci. *29*, 186–191.

Kalinovsky, A., Boukhtouche, F., Blazeski, R., Bornmann, C., Suzuki, N., Mason, C.A., and Scheiffele, P. (2011). Development of axon-target specificity of ponto-cerebellar afferents. PLoS Biol. *9*, e1001013.

Kerjan, G., Dolan, J., Haumaitre, C., Schneider-Maunoury, S., Fujisawa, H., Mitchell, K.J., and Chédotal, A. (2005). The transmembrane semaphorin Sema6A controls cerebellar granule cell migration. Nat. Neurosci. *8*, 1516–1524.

Kuwako, K., Kakumoto, K., Imai, T., Igarashi, M., Hamakubo, T., Sakakibara, S., Tessier-Lavigne, M., Okano, H.J., and Okano, H. (2010). Neural RNA-binding protein Musashi1 controls midline crossing of precerebellar neurons through posttranscriptional regulation of Robo3/Rig-1 expression. Neuron *67*, 407–421.

Li, J., Erisir, A., and Cline, H. (2011). In vivo time-lapse imaging and serial section electron microscopy reveal developmental synaptic rearrangements. Neuron *69*, 273–286.

Manzini, M.C., Ward, M.S., Zhang, Q., Lieberman, M.D., and Mason, C.A. (2006). The stop signal revised: immature cerebellar granule neurons in the external germinal layer arrest pontine mossy fiber growth. J. Neurosci. *26*, 6040–6051.

Mason, C.A., and Gregory, E. (1984). Postnatal maturation of cerebellar mossy and climbing fibers: transient expression of dual features on single axons. J. Neurosci. *4*, 1715–1735.

Niell, C.M., Meyer, M.P., and Smith, S.J. (2004). In vivo imaging of synapse formation on a growing dendritic arbor. Nat. Neurosci. *7*, 254–260.

Osterhout, J.A., Josten, N., Yamada, J., Pan, F., Wu, S.W., Nguyen, P.L., Panagiotakos, G., Inoue, Y.U., Egusa, S.F., Volgyi, B., et al. (2011). Cadherin-6 mediates axon-target matching in a non-image-forming visual circuit. Neuron *71*, 632–639.

Po, M.D., Hwang, C., and Zhen, M. (2010). PHRs: bridging axon guidance, outgrowth and synapse development. Curr. Opin. Neurobiol. *20*, 100–107.

Porter, B.E., Weis, J., and Sanes, J.R. (1995). A motoneuron-selective stop signal in the synaptic protein S-laminin. Neuron *14*, 549–559.

Riehl, R., Johnson, K., Bradley, R., Grunwald, G.B., Cornel, E., Lilienbaum, A., and Holt, C.E. (1996). Cadherin function is required for axon outgrowth in retinal ganglion cells in vivo. Neuron *17*, 837–848.

Sanes, J.R., and Yamagata, M. (2009). Many paths to synaptic specificity. Annu. Rev. Cell Dev. Biol. *25*, 161–195.

Scheiffele, P., Fan, J., Choih, J., Fetter, R., and Serafini, T. (2000). Neuroligin expressed in nonneuronal cells triggers presynaptic development in contacting axons. Cell *101*, 657–669.

Shen, K., and Scheiffele, P. (2010). Genetics and cell biology of building specific synaptic connectivity. Annu. Rev. Neurosci. *33*, 473–507.

Siu, R., Fladd, C., and Rotin, D. (2007). N-cadherin is an in vivo substrate for protein tyrosine phosphatase sigma (PTPsigma) and participates in PTPsigma-mediated inhibition of axon growth. Mol. Cell. Biol. *27*, 208–219.

Sotelo, C. (1975). Anatomical, physiological and biochemical studies of the cerebellum from mutant mice. II. Morphological study of cerebellar cortical neurons and circuits in the weaver mouse. Brain Res. *94*, 19–44.

Sotelo, C. (2004). Cellular and genetic regulation of the development of the cerebellar system. Prog. Neurobiol. *72*, 295–339.

Sotelo, C., and Chédotal, A. (2013). Hindbrain tangential migration. In Cellular Migration and Formation of Neuronal Connections; Comprehensive Developmental Neuroscience, *Volume 2*, J. Rubenstein and P. Rakic, eds. (New York: Academic Press), pp. 345–362.

Sugihara, I. (2005). Microzonal projection and climbing fiber remodeling in single olivocerebellar axons of newborn rats at postnatal days 4-7. J. Comp. Neurol. *487*, 93–106.

Takeichi, M. (2007). The cadherin superfamily in neuronal connections and interactions. Nat. Rev. Neurosci. *8*, 11–20.

Togashi, H., Abe, K., Mizoguchi, A., Takaoka, K., Chisaka, O., and Takeichi, M. (2002). Cadherin regulates dendritic spine morphogenesis. Neuron *35*, 77–89.

Umemori, H., Linhoff, M.W., Ornitz, D.M., and Sanes, J.R. (2004). FGF22 and its close relatives are presynaptic organizing molecules in the mammalian brain. Cell *118*, 257–270.

Waites, C.L., Craig, A.M., and Garner, C.C. (2005). Mechanisms of vertebrate synaptogenesis. Annu. Rev. Neurosci. *28*, 251–274.

White, J.J., and Sillitoe, R.V. (2013). Development of the cerebellum: from gene expression patterns to circuit maps. Wiley Interdiscip. Rev. Dev. Biol. *2*, 149–164.

Williams, M.E., Wilke, S.A., Daggett, A., Davis, E., Otto, S., Ravi, D., Ripley, B., Bushong, E.A., Ellisman, M.H., Klein, G., and Ghosh, A. (2011). Cadherin-9 regulates synapse-specific differentiation in the developing hippocampus. Neuron *71*, 640–655.